Journal of Southeast University (English Edition) Vol. 25, No. 1, pp. 79 – 82 Mar. 2009 ISSN 1003—7985

Numerical simulation of dynamic pore pressure in asphalt pavement

Cui Xinzhuang[1] Jin Qing[1] Shang Qingsen[1] Zhai Jiguang[2]

([1] School of Civil Engineering, Shandong University, Jinan 250061, China)
([2] Haihe Valley Administration Bureau of Shandong Province, Jinan 250100, China)

Abstract: For studying the driving role of dynamic pressure in water-induced damage of asphalt pavement, based on the fast Lagrangian finite difference method and Biot dynamic consolidation theory, fluid-solid coupling analysis of the pavement is conducted considering asphalt mixtures as porous media. Results reveal that the development and dissipation of the dynamic pore pressure are coinstantaneous and this makes both the positive and negative dynamic pore pressure and seepage force alternate with time. Repetitive hydrodynamic pumping and sucking during moisture damage is proved. The dynamic pore pressure increases with vehicle velocity. Effective stress and deflection of pavement decrease due to the dynamic pore water pressure. However, the emulsification and replacement of the asphalt membrane by water are accelerated. The maximum dynamic pore pressure occurs at the bottom of the surface course. So it is suggested that a drain course should be set up to change the draining condition from single-sided drain to a two-sided drain, and thus moisture damage can be effectively limited.

Key words: road engineering; asphalt pavement; moisture damage; dynamic pore pressure; seepage force; dynamic deflection

Many investigations have indicated that much damage such as stripping, pot holes, pumping and cracking occur in asphalt pavement surface only one or two years after opening to traffic, and consequently the inner structure is seriously damaged[1-4]. All the above kinds of damage are called moisture damage. It is important to study moisture damage when considering the design, construction and maintenance of asphalt pavement.

Asphalt membrane is sensitive to being emulsified and replaced by water. At the same time, positive and negative pore water pressure are generated due to repetitive traffic loads, and then water is pumped out and sucked into the asphalt pavement surface course. Under the scouring force of high pressure water, the asphalt membrane is stripped from the aggregate surface. This is the gradually accepted mechanism of moisture damage to asphalt pavement. Dynamic water pressure plays an important role during moisture damage. However, the data in situ regarding dynamic water pressure is scarce. Although Liu et al. [5] attempted to measure it, the peak value of dynamic pore pressure and its total process of development and dissipation were not obtained because the sampling frequency used was too low. Muhammed[6] and Al-Omari et al. [7] used X-ray CT techniques to obtain three-dimensional real pore structures of asphalt concrete specimens, and then numerous steady and unsteady fluid flow simulations were conducted on different asphalt specimens to study the moisture transport characteristics. Kettil et al. [8] used an FEM program to simulate the dynamic pore pressure in pavement structure; however, three-dimensional computation was found to be unstable.

In this regard, employing Biot dynamic consolidation theory and the three-dimensional finite difference method, the dynamic fluid-solid coupling numerical analysis of saturated asphalt pavement is conducted in this paper. Dynamic deflection, dynamic pore pressure and seepage force under single vehicle loads are calculated and the mechanism of the acceleration of moisture damage to dynamic pore pressure is analyzed.

1 Dynamic Fluid-Solid Coupling Theory

In general, when the voidage of asphalt mixture ranges from 8% to 15%, moisture damage is the most serious because it is easy for water to flow into the pavement surface course and difficult to be drained out. In this case, the asphalt mixture can be considered as a porous medium. According to Biot consolidation theory, the dynamic equilibrium equation of the three-dimensional saturated elastic porous medium is

$$G\nabla^2 \boldsymbol{u} + \frac{G}{1-2v}\nabla \operatorname{div}\boldsymbol{u} = \nabla p_{\mathrm{p}} + (1-n)\rho_{\mathrm{s}}\frac{\partial \boldsymbol{v}_{\mathrm{s}}}{\partial t} + n\rho_{\mathrm{f}}\frac{\partial \boldsymbol{v}_{\mathrm{f}}}{\partial t} \tag{1}$$

where $\boldsymbol{u}$ and $\boldsymbol{v}_{\mathrm{s}}$ are the displacement and the velocity vectors of the solid medium, respectively; $\boldsymbol{v}_{\mathrm{f}}$ is the velocity vector of fluid; G, v, n and ρ_{s} are the shear modulus, the Poisson ratio, the voidage and the density of the solid medium, respectively; ρ_{f} is the density of fluid; p_{p} is the pore pressure.

The continuous seepage differential equation is

$$\frac{k}{\gamma_{\mathrm{f}}}\nabla^2 p_{\mathrm{p}} = n\beta_{\mathrm{f}}\frac{\partial p}{\partial t} + \frac{\partial(\operatorname{div}\boldsymbol{u})}{\partial t} \tag{2}$$

where k is the coefficient of permeability; β_{f} is the compression coefficient of fluid; γ_{f} is the bulk density of fluid.

The flowing of fluid causes a scouring force on solid skeletons and this force is referred to as seepage force in continuous porous medium mechanics. Seepage force is a kind of bulk force and on stream line can be expressed as $j = \gamma_{\mathrm{f}} i$, where i is the hydraulic gradient that is water head loss per unit seepage length.

Received 2008-06-26.

Biography: Cui Xinzhuang (1974—), male, doctor, associate professor, cuixz@ sdu. edu. cn.

Foundation items: The National Natural Science Foundation of China (No. 50708056), Reward Fund for Excellent Young and Middle-Aged Scientists of Shandong Province (No. 2008BS09015), the Natural Science Foundation of Shandong Province (No. Q2006F02), Key Technologies R& D Program of Shandong Province (No. 2008GG10006009).

Citation: Cui Xinzhuang, Jin Qing, Shang Qingsen, et al. Numerical simulation of dynamic pore pressure in asphalt pavement[J]. Journal of Southeast University (English Edition), 2009, 25(1): 79 – 82.

2 Material Models and Mechanics Parameters

In China, semi-rigid pavements are widely used. In this paper, a typical semi-rigid pavement is analyzed by the fast Lagrangian finite difference method. We use the elastic constitutive model for the surface course and the base course and the Mohr-Coulomb elastic-plasticity model for embankment soil. The mechanics parameters of all courses of subgrade are shown in Tab. 1. The voidage of the asphalt mixture is 8%. Surface courses are saturated and penetrable by water, but the base course is assumed to be not penetrable.

Tab. 1 Mechanics parameters of all courses of subgrade

Course name	Materials	Thickness/cm	Young's modulus/MPa	c/kPa	ϕ/(°)	Permeability coefficient/ ($\mu m \cdot s^{-1}$)
Upper surface course(USC)	AK-16A asphalt concrete	4	1 148			2.13
Middle surface course(MSC)	AC-25 Ⅰ asphalt concrete	6	984			1.07
Lower surface course(LSC)	AC-25 Ⅰ asphalt concrete	8	820			1.07
Base course(BC)	Cement-stabilized macadam	32	1 500			
Sub-base course(SBC)	Flyash-lime-soil	18	750			
Road bed(RB)	Silty clay	80	42.0	32	20	
Upper embankment(UE)	Silty clay	70	41.4	26	16	
Lower embankment(LE)	Silty clay	100	41.0	23	14	

In analysis, damping is calculated by the Rayleigh linear combination method: $\boldsymbol{C} = \alpha \boldsymbol{M} + \beta \boldsymbol{K}$, where α and β are the constants related to the natural frequency ω and the damping ratio ξ of structure, $\alpha = \xi\omega$, $\beta = \xi/\omega$. According to model analysis, $\omega = 12$ Hz. ξ is taken as 0.01.

3 Wheel Load Model and Boundary Conditions

Wheel loads are simplified as uniform pressure on two circles. The equivalent circle radius δ is 10.65 cm, as shown in Fig. 1. The time history curve of a single wheel load p is shown in Fig. 2 and it can be expressed as[9]

$$p = \begin{cases} p_{\max} \sin^2\left(\dfrac{\pi}{T} t\right) & 0 \leqslant t \leqslant T \\ 0 & t > T \end{cases} \qquad (3)$$

where $p_{\max}$ is the peak value of the load, $p_{\max} = 0.7$ MPa; T is the action time of a single wheel load which has an inverse relationship with the vehicle speed. When the vehicle speed is 80 km/h, T is about 0.045 s.

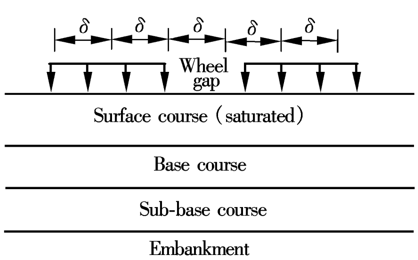

Fig. 1 Wheel load model

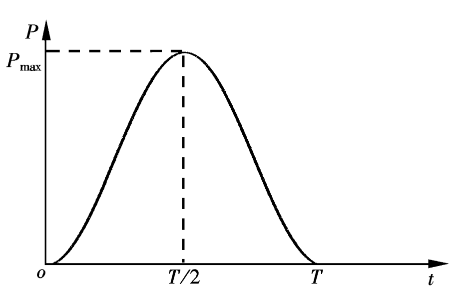

Fig. 2 Time history curve of wheel load

In numerical dynamic calculation, the main error is from the fact that the infinity region is replaced with the finite region. Setting manual boundary is an effective method to decrease this error. The viscous boundary method introduced by Lysmer and Kuhlemeyer[10] was employed on infinite boundaries to absorb the energy of stress waves and prevent stress waves from reflecting.

The interface of the surface course and the base course is impervious, so herein the hydraulic gradient along the vertical direction is zero; i. e. $\partial p_p / \partial z = 0$. On the road face, p_p is zero.

4 Results and Discussion

The finite difference program FLAC (Fast Lagrangian Analysis of Continua) is employed to compute the dynamic deflection, the dynamic pore pressure and the seepage force in asphalt pavement under vehicle loads. The multi-physical field-coupled analysis function of FLAC is powerful, and it has been widely used in civil engineering.

4.1 Dynamic deflection

Defining that the upward deflection of the pavement is positive, time history curves of the deflection under wheel gaps are shown in Fig. 3. It can be seen that the deflection is downward initially and then upward. Because of inertia, it is not $T/2$ when the negative peak value appears, but between $T/2$ and T. The positive peak appears when $t = 2T$ approximately.

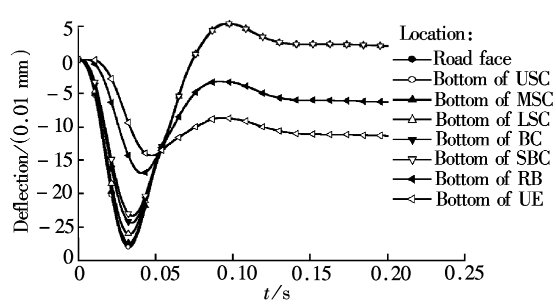

Fig. 3 Time history curves of deflection($T = 0.05$ s)

In order to make a comparison with the case that the surface course is undrained, the permeability coefficient of asphalt concrete is set very small to simulate the undrained case. Fig. 4 shows the influence of draining conditions on road surface deflection. We can see that the absolute peak value of road surface deflection decreases when asphalt concrete is undrained. The reason is that undraining makes the dynamic water pressure increase and consequently the effective stress in the surface course decreases according to the Terzaghi effective stress principle in porous medium mechanics.

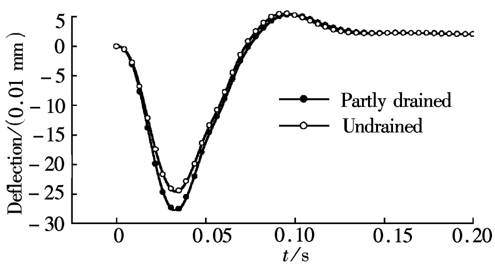

Fig. 4 Effect of draining condition on deflection($T=0.05$ s)

4.2 Dynamic pore pressure

Fig. 5 shows the development and dissipation curves of dynamic pore water pressure under wheel gap. We can see that dynamic water pressure first increases to the positive peak value, then decreases gradually to the negative peak value and at last is turned into hydrostatic pressure. The negative water pressure is also referred to as suction. This calculation result proves the process that water is pumped out and sucked into the pavement surface course repetitively under traffic loads.

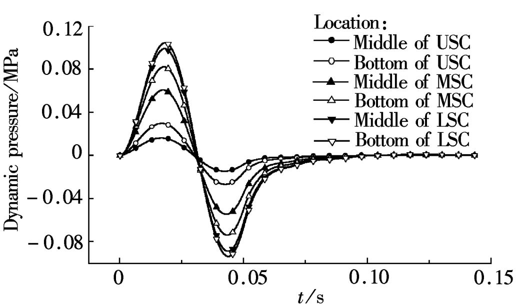

Fig. 5 Time history curves of dynamic pore pressure($T=0.05$ s)

Attenuation curves of water pressure peak values under wheel gap versus depth are shown in Fig. 6 when $T=0.03$, 0.04, 0.05, 0.06, 0.07s, respectively. It can be seen that the smaller T is, the larger the absolute value of dynamic water pressure is. This is because the higher the vehicle speed is, the more the development speed of dynamic pore pressure is than the dissipation speed. Dynamic pore pressure increases with depth and the maximum absolute value appears at the bottom of the surface course. So if a draining course is set at the bottom of the surface course to make single-sided draining conditions turn to double-sided draining conditions, the moisture damage can be limited.

The dissipation of dynamic pore pressure is simultaneous with its development. In order to prove this process, partly drained and totally undrained cases are analyzed numerically, respectively, as shown in Fig. 7. For a totally undrained condition, the shape of the time history curve of dynamic pore pressure is similar to that of the wheel load shown in Fig. 2 and there is no suction. Moreover, the maximum pore

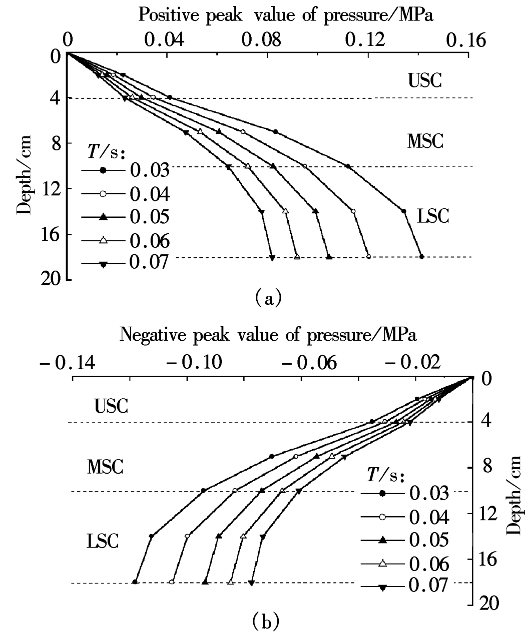

Fig. 6 Vertical attenuation of peak value of dynamic pore pressure. (a) Positive peak value; (b) Negative peak value

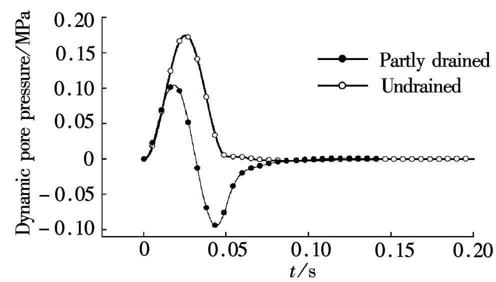

Fig. 7 Effect of drain condition on pore pressure($T=0.05$ s)

pressure is larger than that from a partly drained condition. This implies that developing and dissipating processes are simultaneous. Otherwise, it cannot be obtained that positive and negative pore pressures appear alternately. The simultaneity means that the positive peak value not appear when $t=T/2$, but appears before this time.

Curves of vertical total stress, effective stress and dynamic pressure versus time are shown in Fig. 8. In the initial period of loading, it is difficult for water to flow out. This means that the total stress is mostly borne by water, and, consequently, effective stress is approximately zero. Compared with total stress, the peak value of effective stress decreases and lags due to positive dynamic pressure, and its period is protracted due to negative dynamic pressure.

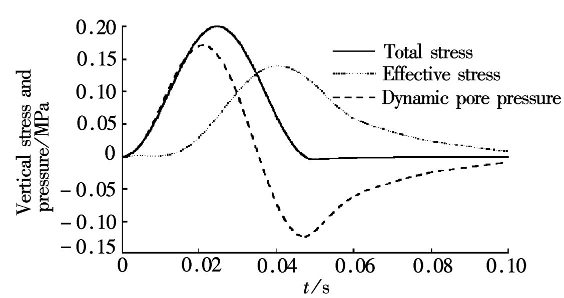

Fig. 8 Time history curves of effective stress and total stress ($T=0.05$ s)

4.3 Seepage force

Time history curves of the seepage force on asphalt mixtures are shown in Fig. 9. Note that the upward seepage force is positive. Positive and negative seepage forces are also alternating and the maximum absolute value of a seepage force appears in the middle surface course.

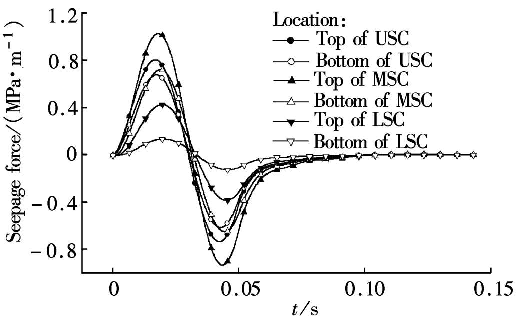

Fig. 9 Variation of seepage force with time

Though dynamic pressure decreases effective stress, the emulsification and replacement of the asphalt membrane by water are accelerated under high pressure water and scouring forces. The asphalt membrane is damaged and scoured out of the pavement surface gradually and at last the aggregates without cohesion are taken away by high speed wheels. This is the total generation process of moisture damage.

5 Conclusions

Dynamic pore pressure plays a significant role in moisture damage of asphalt pavement. However, the generation process of dynamic pressure and its mechanism of accelerating the moisture damage are not very clear. The fast Lagrangian finite difference method and the Biot dynamic consolidation theory are used to analyze the dynamic response of semi-rigid pavement. The analysis reveals the following conclusions:

1) The dissipation of dynamic pore pressure is simultaneous with its development and this is the reason that positive and negative pore pressures appear alternately.

2) Due to dynamic pressure, repetitive seepage force is generated and it scours the damaged asphalt membranes out of the pavement surface. This is the dynamic mechanism of moisture damage.

3) The maximum dynamic pressure and the maximum seepage forces appear at the bottom and the middle of the surface course, respectively.

4) Compared with total stress, the effective stress in the surface course decreases due to dynamic pressure.

References

[1] Kandhal P S. Field and laboratory investigation of stripping in asphalt pavements: state of the art report [J]. *Transportation Research Record*, 1994, **80**(1454): 36 − 47.

[2] Mallick R B, Pelland R, Hugo F. Use of accelerated loading equipment for determination of long term moisture susceptibility of hot mix asphalt [J]. *Int J Pavement Eng*, 2005, **6**(2): 125 − 136.

[3] Chen J S, Lin K Y, Young S Y. Effects of crack width and permeability on moisture-induced damage of pavements [J]. *J Mater Civil Eng*, 2004, **16**(3): 276 − 281.

[4] Masad E, Birgisson B, Al-Omari A, et al. Analytical derivation of permeability and numerical simulation of fluid flow in hot-mix asphalt [J]. *Journal of Materials in Civil Engineering*, 2004, **16**(5): 487 − 496.

[5] Liu Pu, Ling Hongwei, Han Ji. Measurement of pore water pressure in asphalt pavement [J]. *Shanghai Highway*, 2002, **10**(4): 20 − 22. (in Chinese)

[6] Muhammed E K. Modeling moisture transportation in asphalt pavements [D]. Maryland: Department of Civil and Environmental Engineering of University of Maryland, 2005.

[7] Al-Omari A, Masad E. Three dimensional simulation of fluid flow in X-ray CT images of porous media [J]. *Int J Numer Anal Meth Geomech*, 2004, **28**(13): 1327 − 1360.

[8] Kettil P, Engström G, Wiberg N E. Coupled hydro-mechanical wave propagation in road structures [J]. *Computers and Structures*, 2005, **83**(21): 1719 − 1729.

[9] Huang Y H. *Pavement analysis and design* [M]. Delhi: Pearson Education, 1993: 50 − 51.

[10] Lysmer J, Kuhlemeyer R L. Finite dynamic model for infinite media [J]. *Journal of Engineering Mechanics*, 1969, **95**(2): 859 − 877.

沥青路面内动空隙水压力的数值模拟

崔新壮[1]　金　青[1]　商庆森[1]　翟继光[2]

([1] 山东大学土建与水利学院,济南 250061)
([2] 山东省海河流域水利管理局,济南 250100)

摘要:为了研究沥青路面内的动水压力,基于 Biot 固结方程,将沥青混合料看作多孔介质,并考虑了它和水体的惯性力及两者之间的耦合作用,对饱水沥青路面进行了快速 Lagrange 有限差分分析. 结果表明,水压的产生和消散在轮载作用过程中同时存在,导致面层内正负水压力及渗透力随时间交替出现,这证实了水损坏过程中的水力反复泵吸作用. 动孔隙水压力随车速的增大而增大,而且由于水压力的存在路面弯沉和面层内的有效应力减小,但水对沥青膜的乳化和置换作用加强. 动水压力的最大值出现在面层底部,所以建议在面层底部设一排水层,将排水状态由单面排水变为双面排水,有效抑制水损坏的发生.

关键词:道路工程;沥青路面;水损坏;动孔隙水压力;渗透力;动弯沉

中图分类号:TU473.2